Journal of Highway and Transportation Research and Development
2024, 18(4) : 119−127
Research Article
ISSN 2095−6215
DOI：10.26599/HTRD.2024.9480041

Shear hysteresis effects in concrete box girders with simply supported butterfly webs

Yunfei Zhang[1, 2*], Guangru Jiao[2**], Jianbing Chen[2], Xinjiang Cai[2]

1. *Tongzhou Branch of Jiangsu Joint Vocational Technical College, Nantong, Jiangsu 226000, China*;
2. *School of civil Engineering, Suzhou University of Science and Technology, Suzhou, Jiangsu 215011, China*

Abstract: The butterfly web concrete box girder represents an innovative bridge structure characterized by a hollow butterfly web design. This structure is noted for its lightweight nature, reduced maintenance costs, and abbreviated construction timelines. To investigate the distribution of the shear hysteresis effect, a test beam model of the butterfly web was conceptualized and constructed. Subsequently, static loading tests were conducted, and a corresponding ABAQUS finite element model was developed to align with the experimental conditions. Utilizing the principle of section equivalence, a calculation method for the moment of inertia (Ik) at the hollow web of the box girder was proposed. Furthermore, a formula for determining the shear hysteresis effect of the butterfly web box girder was established through the application of the energy variation method. The findings from the experimental, finite element, and theoretical analyses indicate that the shear hysteresis effect at the hollow web of the butterfly web box girder surpasses that of the solid web. Additionally, the shear hysteresis effect is most pronounced at the intersection of the web and the top plate, diminishing progressively towards the edges. The shear hysteresis effect is also more significant at the supporting and span sections of the box girder. The longitudinal stress values derived from the variational method exhibit an error range of −2.4% to 7.4% when compared to test values under concentrated loads, and a similar error range of −2.4% to 7.4% when compared to finite element values under uniform loads. The discrepancies between the longitudinal stress values and the finite element values range from −2.7% to 3.8%, thereby validating the accuracy of the proposed formula. The outcomes of this research may serve as a valuable reference for the design of butterfly web box girders.

Keywords: bridge engineering; butterfly web box girder; shear hysteresis effect; energy variational method; finite element

1 Introduction

The butterfly web concrete box girder is a new form of bridge structure with the advantages of light weight, low maintenance cost, short construction period and beautiful shape compared to the traditional concrete box girder[1]. The main feature of this structure is the butterfly shaped web, which is similar to the “X” shaped double layer Warren truss structure[2]. The load is divided into areas of principal compressive stress and areas of principal tensile stress. In addition, high-strength steel fibre concrete was used for the web material, with the aim of preventing cracks in the main tensile stress area of the web, which could lead to web failure.

The world’s first butterfly web box girder bridge, the Tagubo River Bridge, was completed by Japan in 2013, as shown in Figure 1. Japanese scholars have conducted a series of studies on this structure, Akio Kasuga[2] carried out wind tunnel tests on a butterfly web box girder structure to investigate its wind resistance performance; Yuki Kaminaga[3] introduced the construction method, web construction and force transfer method of butterfly web concrete box girder structure using the Akutagawa Bridge as the research object, and verified through finite

Received: 26 December 2023; **Revised:** 10 March 2024; **Accepted:** 22 June 2024
* *E-mail address*: zyf0867@foxmail.com
** *Corresponding author*: szctt2009@163.com

Translated from *Journal of Highway and Transportation Research and Development* (Chinese, ISSN1002-0268), 2024, 41(9): 123−131.

Fig. 1 The takubogawa bridge

element model that the web transfer method is similar to that of a double-layer Warren truss structure.

The butterfly web is novel in terms of structural form and force transmission mechanism but there are no real bridges in China and little research has been done on its mechanical properties. In order to study the mechanical properties of butterfly web box girders, Jiao Guangru[4] made a test model of a butterfly web box girder and loaded the model symmetrically at three points, the test results showed that under the vertical load, there was a large shear deformation at the location of the butterfly web joints, but the box girder as a whole still had good flexural performance. Zhu Zihao[5] derived a formula for calculating the shear deformation of butterfly webs, verified the accuracy of the theoretical formula through finite elements, and changed the thickness of the web and the magnitude of the tensile stress in the direction of the main tensile stress on the basis of the finite element model to analyse the relationship between the two and the shear deformation of the web, and the study showed that increasing the thickness of the web and applying prestress could effectively improve the web bearing capacity.

2 Models and tests

2.1 Specimen design

The butterfly web box girder model has a total length of 3 570 mm, a calculated span of 3 400 mm, a beam height of 480 mm, a web height of 430 mm and a plate thickness of 50 mm. the top and bottom plate widths are 880 mm and 550 mm respectively and the plate thicknesses are both 80 mm[6]. The specific dimensions of the box girder are shown in Figure 2.

The web section is a hollowed-out butterfly shape with a total of 16 webs used on both sides, as shown in Figure 2(a). Each web is spaced 10mm apart and is

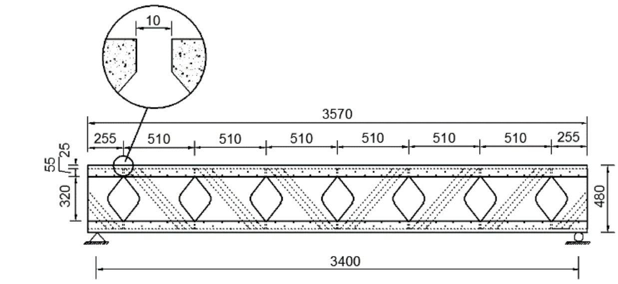

(a) Elevation of the model beam

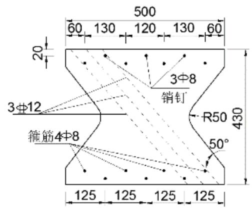

(b) Web dimensions

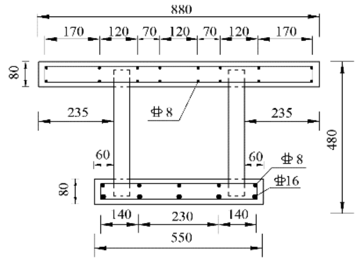

(c) Cross-sectional drawing of box girder

(d) Web assembly drawing

(e) Test beam model

Fig. 2 Structure diagram of butterfly web box girder (unit: mm)

precast in C60 steel fibre concrete (1.75% steel fibre by volume), the purpose of which is to prevent premature cracking in the main tensile stress area of the web and to resist the main tensile directional stresses together with the web reinforcement, the specific dimensions of the webs are shown in Figure 2(b). The webs are connected to the top and bottom slabs using 8 mm diameter HPB300 grade hoop bars as well as pins, both of which act as shear connectors. Three 12-mm diameter HRB400 grade reinforcement bars with a spacing of 50mm are placed in the direction of the main tensile stress in the web, and the sloping angle of the hollow section of the web is 50°[7]. The top and bottom slabs were cast in C30 ordinary concrete with double reinforcement, with the top slab reinforced according to the structural requirements and the bottom slab reinforced with 8 mm diameter HRB400 grade reinforcement at the top and 16 mm diameter HRB400 grade reinforcement at the bottom, as shown in Figure 2(c). The prefabricated webs are assembled as shown in (Figure 2(d)) and finally the top and bottom slabs of the box girder are poured and shaped as shown in (Figure 2(e)). The measured modulus of elasticity of C60 steel fibre concrete is 3.58×10^4 MPa, The modulus of elasticity of C30 plain concrete is 2.93×10^4 MPa.

2.2 Location of measurement points

Sections A and B of the test beam were selected for the study, and a total of 28 measurement points were arranged on the top and bottom plates of the box beam, of which 18 points were arranged on the top plate and 10 points on the bottom plate. The specific arrangement of measurement points and section selection are shown in Figure 3.

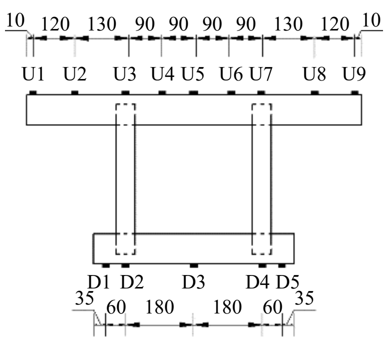

(a) Cross-sectional measurement point layout

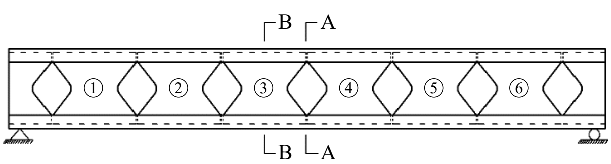

(b) The measurement points are arranged in section along the length of the beam

Fig. 3 Arrangement of strain gage (unit: mm)

2.3 Loading options

The test beam was loaded symmetrically at three points in the test beam, which was simply supported and loaded in the position shown in Figure 4. The data was collected by the DH382NET static strain test system and the loading process was displacement-controlled, with 0.5 mm displacement levels loaded in steps.

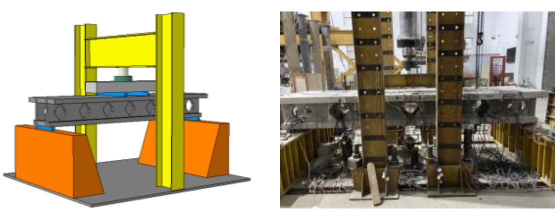

Fig. 4 Loading mode of model beam

2.4 Analysis of test results

The actual longitudinal strains collected were converted to longitudinal stresses according to the stress-strain relationship and the actual measured modulus of elasticity of the material. The distribution of longitudinal stresses in sections A and B under each level of loading is shown in Figures 5 and 6, where the tensile stress is positive and the compressive stress is negative. As can be seen from the figure, the shear hysteresis effect at both the hollow web and the solid web increases with the increase of load, and shows a positive shear hysteresis effect distribution; as the flexural stiffness of the section at the hollow web is lower, which leads to a larger stress value than that at the solid web; the concrete of the bottom slab reaches the yield strength earlier in the process of vertical loading, the concrete withdraws from the force, and the tensile stress begins to be gradually borne by the reinforcement, resulting in a stress redistribution phenomenon, leading to a larger stress in the bottom slab. The stresses in the bottom slab are larger.

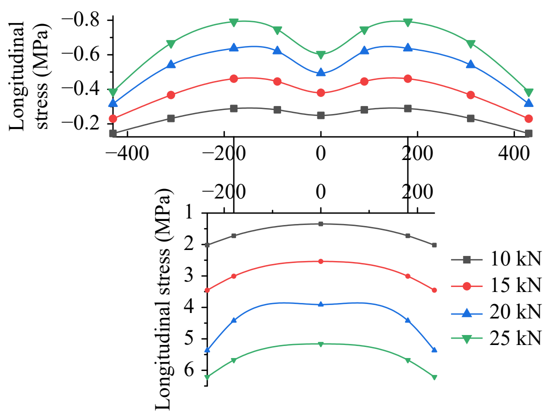

Fig. 5 Longitudinal stress distribution of section A

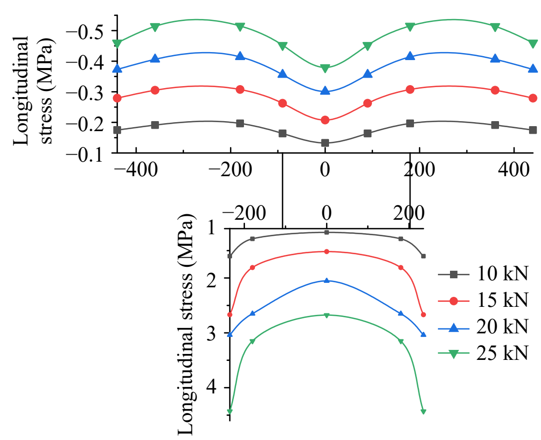

Fig. 6 Longitudinal stress distribution of section B

3 Finite element analysis

3.1 Spatial finite element modeling

The model was simulated using two different types of cells, with solid cells (C3D4R) for the concrete top, bottom and web slabs and line cells (T3D2) for the reinforcement skeleton, for a total of 41 556 cells[8].

The reinforcement skeleton is constrained by Embedded region, the connection between the web and the top and bottom plate is constrained by Tie, the loading pad and the support are constrained by Tie[9], the boundary conditions are consistent with the test, the finite element model is shown in Figure 7.

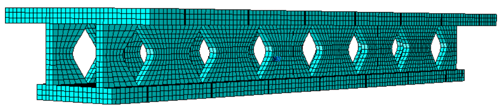

Fig. 7 Finite element model

3.2 Three-dimensional distribution of shear hysteresis effects

Using the advantages of finite element software modelling analysis, the spatial stress state of the butterfly web box beam can be seen more intuitively. By extracting the actual stresses in each section of the FEM model of the butterfly web box beam, the distribution of the shear hysteresis coefficient, i.e. the three-dimensional distribution of the shear hysteresis effect, is calculated and shown in Figures 8 and 9.

As can be seen from the figure, the butterfly web box girder shows a positive shear hysteresis effect distribution under both uniform and concentrated loads. In terms of load form, the shear hysteresis effect under concentrated load is more obvious than under uniform load; in terms of transverse distribution, the shear hysteresis effect is greater at the intersection of the web and top plate and decreases from the ribs to both sides; in terms of longitudinal distribution, the shear hysteresis effect is greater at the pivot section and the span section.

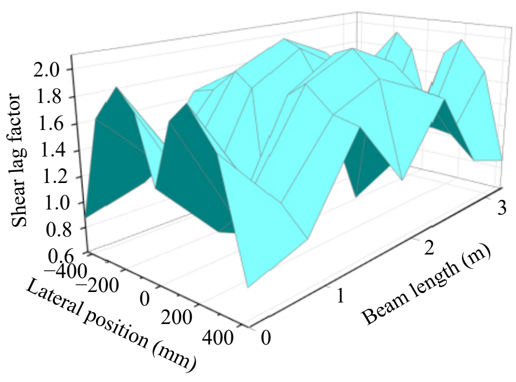

Fig. 8 three-dimensional distribution of shear lag effect under concentrated load

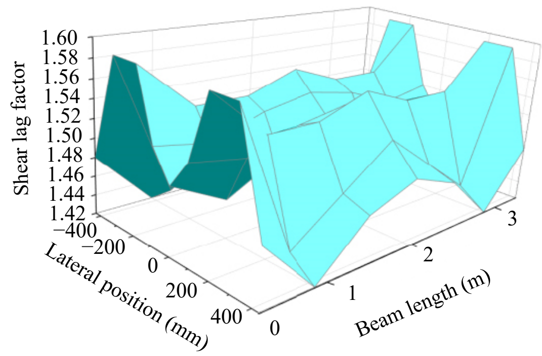

Fig. 9 Three-dimensional distribution of shear lag effect under uniformly distributed load

4 Energy variation method

4.1 Basic assumptions

To establish the shear hysteresis effect control differential equations for concrete box girders with butterfly webs, the following assumptions were made[10-11].

(1) The strain in the cross-section of the structure along the height of the beam under vertical loading of a butterfly web box girder satisfies the assumption of a flat section.

(2) The test beam performed well in the elastic phase with the top and bottom plates working in tandem with the butterfly web.

(3) Ignore the relative slip between the butterfly web and the concrete top and bottom slabs.

4.2 Section equivalents at the hollow web

Based on the principle of equal area and moment of inertia before and after section equivalence, the hollow web portion of the butterfly web is equated to a rectangle, as shown in Figure 10. The web height is h_w, web thickness is t_w, opening height is d, S_1 is spacing at the narrowest part of the web, opening spacing is d_1, the area of the hollow part is A_1, the moment of inertia is I_1, the height of the rectangle at the hollow after area equivalence is h_k, the width is b_k. By the principle of equal area and moment of inertia before and after equivalence[12-13] it follows that $h_k = 2\sqrt{3}i_1$, $b_k = \dfrac{\sqrt{3}A_1}{6i_1}$, $i_1 = \sqrt{\dfrac{I_1}{A_1}}$.

The cross section at the hollow after equivalence is shown in Figure 11. Top plate thickness is t_u, base plate

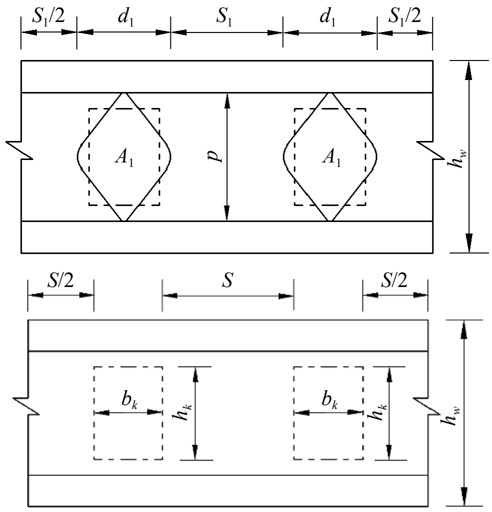

Fig. 10 Equivalent size of butterfly web box girder

thickness is t_c. By substituting h_k and b_k into the hollow web of the box girder cross-section, the moment of inertia I_k in the hollow web of the butterfly web box girder cross-section can be calculated as

$$I_k = \frac{b_t t_u^3}{12} + y^2 t_u b_t + \frac{b_c t_b^3}{12}(h-y)^3 t_b b_c + 4I_0. \tag{1}$$

where, y is the distance from each section to the form centre; the rectangular area at the rib is s and the moment of inertia is I_0.

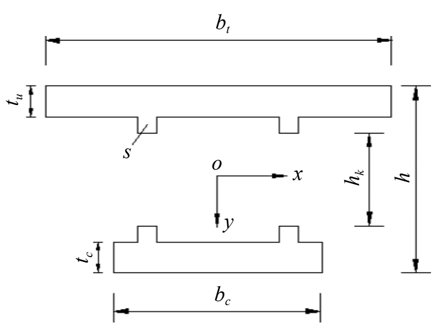

Fig. 11 Equivalent cross section at fasting

4.3 Longitudinal warpage displacement function

In this paper, the shear hysteresis warp displacement function is of cubic parabolic type[14-16]

$$u(x,y) = h_i[\omega'(x) + f(y)U(x)] \tag{2}$$

Where, $\omega'(x)$ is the vertical bending deflection; $U(x)$ is the shear hysteresis generalised displacement; $f(y)$ is the shear hysteresis warpage displacement function; h_i is the distance from the top and bottom plates to the section form centre after section equivalence; $u(x, y)$ is the longitudinal displacement at any point of the box girder section. The specific dimensions and coordinate system of the box girder are shown in Figure 12.

Based on the dimensional form of the top, bottom and flange plates, express $f(y)$ in Equation (2) as

$$f(y) = \begin{cases} -\left[1-\left(\frac{y^3}{b_1^3}\right)\right] & \text{Roof plate} \\ -\left[1-\left(\frac{(b_1+b_2-y)^3}{b_2^3}\right)\right] & \text{Flange plate} \\ 1-\left(\frac{y^3}{b_3^3}\right) & \text{Base plate} \end{cases}. \tag{3}$$

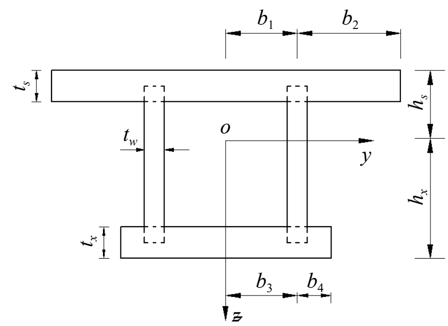

Fig. 12 Size and coordinate system of box girder

4.4 Control differential equations

From the principle of minimum potential energy, it follows that the external forces on the beam in its elastic state satisfy the equilibrium conditions. Of all the displacements that satisfy the boundary conditions, there must be a set of displacements that minimise the total potential energy of the whole system[17-19]. i.e. the first order variation of the total potential energy of the system is zero.

$$\delta\Pi = \delta\left(\overline{U} + \overline{V}\right) = 0, \tag{4}$$

where, Π is the total potential energy of the system; $\overline{U}$ is the strain energy of the system; $\overline{V}$ is External potential energy.

Strain energy of the system:

$$\overline{U} = \frac{1}{2}\int_v (E\varepsilon^2 + G\gamma^2)\mathrm{d}U. \tag{5}$$

The external potential energy when the beam is bent is

$$\overline{V} = -\int_0^l M(x)\frac{\mathrm{d}^2\omega}{\mathrm{d}x^2}\mathrm{d}x. \tag{6}$$

The strain energy of the airfoil and web can be expressed separately as $\overline{U}_s$, $\overline{U}_w$, $\overline{U} = \overline{U}_s + \overline{U}_w$.

The airfoil strain energy is divided into three parts: the top plate, the top airfoil plate and the bottom plate, can be expressed as $\overline{U}_{si}(i = 1, 2, 3)$. The specific expressions are:

$$\sum \overline{U} = \sum_{i=1}^{3} \overline{U}_{si} + \overline{U}_{w} = \overline{U}_1 + \overline{U}_2 + \overline{U}_3 + \overline{U}_{w}. \quad (7)$$

The expression for the strain energy of the airfoil is

$$\sum \overline{U}_{si} = \sum \frac{1}{2} \iint t_i (E\varepsilon_j^2 + G\gamma_j^2) \mathrm{d}x\mathrm{d}y \; (i = s,\ x;\ j = 1,\ 2,\ 3). \quad (8)$$

where, $\varepsilon = \partial u / \partial x$, $\gamma = \partial u \partial y$.

The expression for the strain energy of the web is

$$\overline{U}_{w} = \frac{1}{2} \int_0^l EI_w \left(\frac{\mathrm{d}^2 \omega}{\mathrm{d}x^2} \right) \mathrm{d}x, \quad (9)$$

where, I_w is moment of inertia of the web to the section form centre.

Substituting Equations (8) and (9) into Equations (7) gives

$$\sum \overline{U} = \sum \frac{1}{2} \iint t_i (E\varepsilon_j^2 + G\gamma_j^2) \mathrm{d}x\mathrm{d}y + \frac{1}{2} \int_0^l EI_w \left(\frac{\mathrm{d}^2 \omega}{\mathrm{d}x^2} \right) \mathrm{d}x. \quad (10)$$

Substituting Equations (6) and (10) into Equations (2) gives

$$\delta\left(\sum \frac{1}{2} \iint t_i \left(E\varepsilon_j^2 + G\gamma_j^2 \right) \mathrm{d}x\mathrm{d}y + \frac{1}{2} \int_0^l EI_w \left(\frac{\mathrm{d}^2}{\omega} \mathrm{d}x^2 \right) \mathrm{d}x - \int_0^l M(x) \frac{\mathrm{d}^2 \omega}{\mathrm{d}x^2} \mathrm{d}x \right) = 0. \quad (11)$$

The shear lag differential equation and boundary conditions are solved as

$$\begin{cases} EI\omega'' + 3EI_s U'/4 + M(x) = 0, \\ -9EI_s U''/14 - 3EI_s \omega''''/4 + 9GI_s U/(5b^2) = 0, \\ (9EI_s U'/14 + 3EI_s \omega'')\delta\, U|_{x_1}^{x_2} = 0, \end{cases} \quad (12)$$

where, I_s is Moment of inertia of the airfoil to the section form centre; I is full section bending moment of inertia, $I = I_s + I_w$.

From Equation (12), it follows that

$$\frac{\mathrm{d}^2 U}{\mathrm{d}x^2} - k^2 u = \frac{7nQ(x)}{6EI}. \quad (13)$$

The solution is:

$$U(x) = \frac{7n}{6EI}(C_1 \mathrm{sh}kx + C_2 \mathrm{ch}kx + u^*), \quad (14)$$

where, $n = \dfrac{1}{1 - \dfrac{7I_s}{8I}}$, $k = \dfrac{1}{b}\sqrt{\dfrac{14Gn}{5E}}$; C_1, C_2 are determined by boundary conditions; u^* is special solutions related to the shear force $Q(x)$.

4.5 Equation for calculating normal stress

The stress in the airfoil considering the effect of shear hysteresis is shown in Equation (15).

$$\sigma(x,y) = E\frac{\partial u(x,y)}{\partial x} = Eh_i\left[\frac{M(x)}{EI} + (f(y) + \frac{3I_S}{4I})u' \right]. \quad (15)$$

The loading diagram for a simply supported beam under concentrated load is shown in Figure 13.

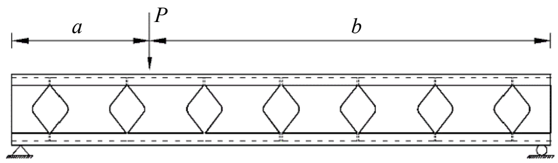

Fig. 13 Schematic diagram of concentrated loading of simply supported beams

Substituting Equation (3) and the parameters n and k into Equation (15) yields the section stress calculation equation as when $0 \leqslant x \leqslant a$,

$$\sigma(x,y) = \frac{h_i}{I}\left\{ M(x) - \frac{7nP}{6k}\left[f(y) - \frac{3I_s}{4I} \right]\left[\frac{\mathrm{sh}k(l-a)}{\mathrm{sh}kl} \mathrm{sh}kx \right] \right\}. \quad (16)$$

When $a < x \leqslant L$,

$$\sigma(x,y) = \frac{h_i}{I}\left\{ \begin{matrix} M(x) - \dfrac{7nP}{6k}\left[f(y) - \dfrac{3I_s}{4I} \right] \\ \times(\mathrm{sh}ka \times \mathrm{ch}kx - \mathrm{sh}ka \times \mathrm{cth}kl \times \mathrm{sh}kx) \end{matrix} \right\}. \quad (17)$$

When $x = 1/2L$,

$$\sigma(x,y) = \frac{h_i}{I_k}\left\{ M(x) - \frac{7nP}{6k}\left[f(y) - \frac{3I_s}{4I_k} \right] \times \frac{\mathrm{sh}(kl/2)}{\mathrm{sh}kl} \mathrm{sh}kx \right\}. \quad (18)$$

The shear hysteresis coefficient of the mid-span section is

$$\lambda = 1 - \frac{7n}{3kl}[f(y) - 3I_s/4I_k]\tan(kl/2), \quad (19)$$

where I_k is moment of inertia of the section at the hollow web.

A schematic diagram of the loading of a simply supported beam under uniform load is shown in Figure 14.

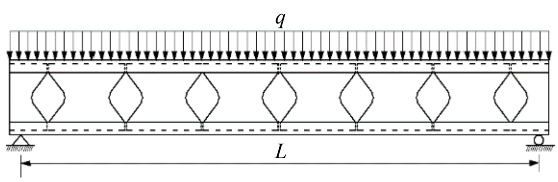

Fig. 14 Schematic diagram of uniformly distributed loading of simply supported beams

Substituting Equation (3) and the parameters n and k into Equation (15) yields the section stress calculation equation as

$$\sigma(x,y)=\frac{h_i}{I}\left\{M(x)-\frac{7nq}{6k^2}\left[f(y)-\frac{3I_s}{4I}\right]\left(1-\mathrm{ch}kx+\frac{\mathrm{ch}kl-1}{\mathrm{sh}kl}\mathrm{sh}kx\right)\right\}. \quad (20)$$

The shear hysteresis coefficient of the mid-span section is

$$\lambda=1-\frac{28n}{3k^2l^2}\left[f(y)-\frac{3I_s}{4I_k}\right]\left[1-\frac{1}{\mathrm{ch}(kl/2)}\right]. \quad (21)$$

5 Comparative analysis

5.1 Comparison of shear hysteresis effects under concentrated loads

Based on the finite element and theoretical equations, the stress values and shear hysteresis coefficients of the top and bottom slabs of the mid-span section under concentrated load were obtained and compared with the experimental values, as shown in Table 1. As the concrete yields earlier under the vertical load in the bottom slab and the tensile stress is carried by the reinforcement, different loads were selected for the top and bottom slabs for analysis to ensure the accuracy of the results, where P_u = 20 kN and P_d = 5 kN. After collating the data in Table 1, the longitudinal stresses in the spanwise cross section of the top and bottom slabs are plotted separately as shown in Figures 15 and 16.

As can be seen from the graphs, the three agree well and all reflect the distribution of shear hysteresis effects in butterfly web box girders under concentrated loads. Among them, the finite element stress value is closer to the test value, and the error between them is 1.2%−5.9%; The error between the stress values of the variational method and the test values ranges from −2.4% to 7.4%; The maximum shear hysteresis coefficient is located at the flange of the bottom slab and the value is large due to the higher actual tensile stress in the bottom slab, the low

Table 1 Comparison of stress value and shear lag coefficient of section A of butterfly web box girder under concentrated load

Location of measurement points	Load (kN)	Theoretical stress values for primary beams (MPa)	Horizontal position (mm)	Stress values (MPa)			Shear lag factor λ		
				Test value	Finite element	Variable Score Method	Test value	Finite element	Variable Score Method
Roof plate	20	−0.42	0	−0.49	−0.51	−0.48	1.23	1.19	1.15
			90	−0.62	−0.64	−0.61	1.53	1.49	1.46
			180	−0.64	−0.65	−0.66	1.56	1.53	1.58
			310	−0.54	−0.56	−0.58	1.36	1.30	1.39
			430	−0.31	−0.32	−0.33	0.78	0.76	0.79
Base plate	5	0.32	0	0.35	0.36	0.37	1.07	1.10	1.13
			180	0.51	0.54	0.53	1.56	1.65	1.63
			235	0.84	0.85	0.82	2.57	2.60	2.51

Note: Tensile stresses are positive and compressive stresses are negative in the table.

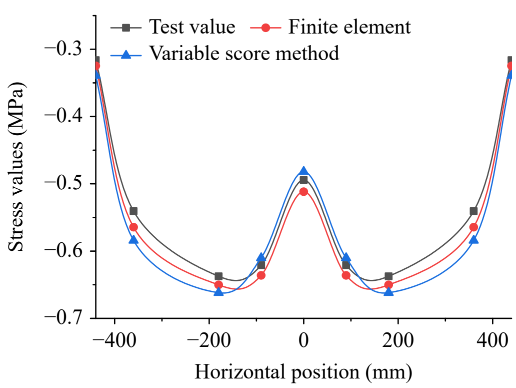

Fig. 15 Comparison of roof stress in section A under concentrated load

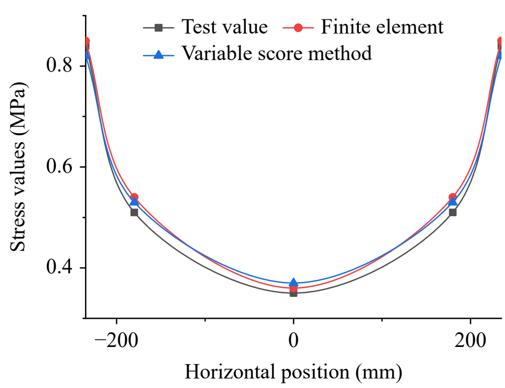

Fig. 16 Comparison of bottom stress in section A under concentrated load

flexural stiffness of the hollow web section in the span and the higher stress value under the primary beam theory, resulting in a large shear hysteresis coefficient. Therefore, in practical works, the bottom slab of the section at the hollow web needs to be reinforced.

5.2 Comparison of shear hysteresis effects under uniform load

In order to study the shear hysteresis effect of the structure under uniform load, the theoretical calculated values were compared with the finite element values and the data was obtained as shown in Table 2. q = 10 kN/m was chosen as the uniform load rating and the data in Table 2 was collated and the longitudinal stresses in the spanwise sections of the top and bottom slabs were plotted as shown in Figures 17 and 18 respectively. As can be seen from the graphs, the variation trends of the finite element and the variational method are consistent and in good agreement, and both can reflect the distribution of the shear hysteresis effect of the structure under uniform loading. The maximum shear hysteresis coefficient is located at the junction of the web and the top plate, and decreases gradually towards the sides.

6 Conclusion

This paper combines experimental, finite element and theoretical methods to study the shear hysteresis effect in butterfly web box girders and concludes as follows.

(1) Under concentrated loads, the longitudinal stresses in the top and bottom plates of the butterfly web box girder show a positive shear hysteresis effect distribution, and the shear hysteresis effect is more obvious in the hollow web than in the solid web.

(2) Under different loads, the shear hysteresis effect along the length of the beam is greater at the pivot section and the mid-span section, while the shear hysteresis effect along the width of the beam is greater at the inter-

Table 2 Comparison of stress value and shear lag coefficient of section A of butterfly web box girder under uniform distributed load

Location of measurement points	Load	Theoretical stress values for primary beams (MPa)	Horizontal position/(mm)	Stress values (MPa)		Shear lag factor λ	
				Finite element	Variable Score Method	Finite element	Variable Score Method
Roof plate	10	−0.50	0	−0.75	−0.73	1.5	1.46
			90	−0.76	−0.75	1.52	1.50
			180	−0.79	−0.82	1.58	1.64
			310	−0.78	−0.80	1.56	1.60
			430	−0.77	−0.78	1.54	1.56
Base plate	10	1.12	0	1.06	1.06	0.95	0.95
			180	1.22	1.20	1.09	1.08
			235	1.32	1.31	1.18	1.18

Note: Tensile stresses are positive and compressive stresses are negative in the table.

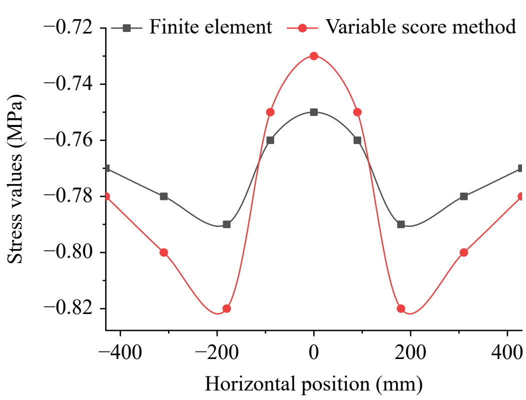

Fig. 17 Comparison of roof plate stress in section A under uniformly distributed load

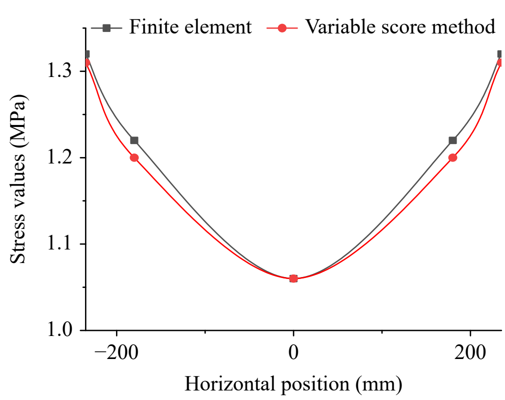

Fig. 18 Comparison of bottom plate stress in section A under uniformly distributed load

section of the web and the top plate, and gradually decreases to the sides.

(3) Based on the principle of equivalent section, the formula for calculating the moment of inertia Ik of the section at the hollow web of the box girder is given, and combined with the energy variation method, the calculation method of shear hysteresis effect of box girder is proposed.

The results show that the error between the longitudinal stress value of the variational method and the finite element value under concentrated load is between −2.4% and 7.4%, and the error between the longitudinal stress value of the variational method and the finite element value under uniform load is between −2.7% and 3.8%. Therefore, the method of this paper is suitable for the calculation of shear hysteresis effects in butterfly web box girders.

Declaration of competing interest

The authors have no competing interests to declare that are relevant to the content of this article.

Acknowledgements

This work was supported in part by the National Natural Science Foundation of China Projects (No. 51778395) and Jiangsu Postgraduate Research and Practice Innovation Program Project (No. SJCX21_1389, No. SJCX19_0837).

References

[1] Kasuga, A. Butterfly web effects on bridge design[J]. Structural Concrete, 2016, 18(1). DOI: 10.1002/suco.201600109.

[2] Kasuga, A. Effects of butterfly web design on bridge construction (Reprinted from Struct[J]. Structural Concrete Journal of the Fib, 2017, 18: 128–142.

[3] Huang, R.Y., Kaminaga, Y., Ashizuka, K., et al. Design and Construction of Butterfly Web Bridge-Akutagawa Bridge[J]. Journal of China & Foreign Highway, 2017, 37(3): 149–151.

[4] Jiao, G.R., Chen, J.B., Zhang, Y.F. Study of Bending Performance of Precast Butterfly Web Concrete Box Girders[J]. China Concrete and Cement Products, 2021(5): 43–47.

[5] Zhu, Z.H., Chen, J.B., Jiao, G.R. Calculation and analysis of shear deformation of butterfly web[J]. Journal of Suzhou University of Science and Technology Engineering and Technology edition, 2021, 34(2): 39–43.

[6] Jiao, G.R. Theoretical Analysis and Experimental Research on the FlexuralPerformance of Concrete Box Girder with Butterfly Webs Theoretical Analysis and Experimental Research with Butterfly Webs[D]. Suzhou: Suzhou University of Science and Technology, 2021.

[7] Zhang, Y.F. Analysis and experimental study on shear lag effect of concrete box girder with butterfly webs[D]. Suzhou: Suzhou University of Science and Technology,2021.

[8] Song T.Y. Full-process shear lag effect of prestressed concrete T-beam based on Abaqus[J]. Journal of Highway and Transportation Research and Development, 2023, 40(6): 103−112.

[9] Zhang L.Z., Cao P.H. Mechanical properties of PC box girders reinforced by secondary stress bonded steel[J]. Journal of Highway and Transportation Research and Development, 2023, 40(10): 79−86.

[10] Qin, Y.Y., Liu, S.Z., Ma, C., et al. Study on Shear Lag Effect of Single-box Twin-cell Corrugated Steel Web-Steel Floor-Concrete Roof Composite Box Girder[J]. Journal of Highway and Transportation Research and Development, 2020, 37(10): 98–106.

[11] Ma, C., Liu, S.Z., Ji, W. Study on Shear Lag Effect of Single-box Multi-cell PC Composite Box Girder with Corrugated Steel Webs[J]. Journal of Highway and Transportation Research and Development, 2018, 35(2): 62–71,78.

[12] Jiang, S., Chen, S.X., Guo, M.H. Research on calculation of equivalent stifiness of octagonal hole castellated beamsJ Engineering Journal of Wuhan University, 2013, 46(S1) 152–159.

[13] Huang, B.S., Huang, T.J., Wang, W.C., et al. Calculation method of equivalent bending stiffness of castellated beams and analysis of its influence factors[J]. Journal of Building Structures, 2018, 39(S2): 121–127.

[14] Chen, Y.L., Liu, S.Z. Shear lag shear effect of single-box and double-cell thickened wing plate CSW simply supported box girder[J]. Journal of Railway Science and Engineering, 2021, 18(10): 2640–2650.

[15] Gao, L., Zhou, Y., Wang, S.L., et al. Energy-variational method of shear-lag effect in PC box-girder with corrugated steel webs[J]. Journal of Xi'an University of Architecture and Technology (Natural Science Edition), 2022, 54(1): 27–34.

[16] Luo, M., Lin, P.Z., Yang, Z.J., et al. Analysis of shear lag effect of box girder under different section forms[J]. Chinese Journal of Applied Mechanics, 2021, 38(5): 2092–2097.

[17] Wu, Q.M., Jiang, R.J., Xu, T.H., et al. Analysis on shear-lag effect of composite box girders with corrugated steel webs considering shear deformation of webs[J]. Journal of Building Structures, 2021, 42(S1): 220–228.

[18] Li, X.Y., Guo, J.Y., Wan, S., et al. Analysis on Shear Lag Effect of Thin-walled Box Girder Based on Timoshenko Beam Theory[J]. Journal of Highway and Transportation Research and Development, 2018, 35(6): 52–60,94.

[19] Luo, M., Lin, P.Z., Sun, L.X. Experimental study on shear lag effect of twin-cell box girder[J]. Railway Engineering, 2015(10): 56–59.